Clays and Clay Minerals, Vol. 42, No. 2, 197–206, 1994.

REACTION PATH APPROACH TO MINERAL WEATHERING REACTIONS

PHILIPP STEINMANN, PETER C. LICHTNER,[1] AND WILLIAM SHOTYK
Geological Institute, University of Berne, Baltzerstrasse 1, CH-3012 Berne, Switzerland

Abstract—Commercial spreadsheet programs allow calculation of reasonable reaction paths for weathering of silicate minerals in a dilute acidic aqueous solution. These calculations use reaction coefficients of simplified weathering reactions and ignore speciation in the aqueous solution. The method is illustrated using the example of dissolution of microcline. When plotted on a log-log activity diagram, the obtained reaction paths are clearly curved, unlike the straight lines shown in most recent geochemistry textbooks. The calculated reaction paths are strongly dependent on the initial pH of the solution. At higher pH the speciation in the solution must be included in the calculations. The most important speciation reactions (the dissociation of H_2O and H_4SiO_4) can be easily included using commercial mathematical programs.

The presented examples include closed systems with different initial pH values and an open system case describing the evolution of a soil profile. All reaction paths calculated using the simplified methods agree well with those obtained using sophisticated modeling codes.

Key Words—Geochemical modeling, Gibbsite, Kaolinite, Microcline, Reaction path, Weathering.

INTRODUCTION

The chemical composition of natural waters, soils, and sediments are to a large extent controlled by water-rock interactions. Primary alumosilicate minerals formed in the earth crust are unstable when exposed to H_2O, O_2, and CO_2 in the atmosphere. They decompose, releasing dissolved salts and forming new, more stable, secondary minerals.

Reaction path modeling of such mineral weathering reactions was introduced by Helgeson (1968). In a companion paper, Helgeson *et al.* (1969) gave a lucid example of the reaction path taken by potassium feldspar dissolving in pure water at 25°C and 1 atm. Originally formulated with the computer code PATH, the reaction path concept has served as a useful tool for studying geochemical problems involving fluid-rock interaction. Since then there have been numerous applications, with subsequent development of more sophisticated codes such as EQ3/6 (Wolery and Daveler, 1992), MPATH (Lichtner, 1992) NETPATH (Plummer *et al.*, 1991) and others.

Several recent geochemistry textbooks have discussed reaction paths using examples taken from Helgeson's work. In contrast to the clarity of the original discussion, the textbook examples are either misleading or incorrect. Stumm and Morgan (1981), for example, omit important details at mineral stability boundaries. In the books by Berner and Berner (1987), Richardson and McSween (1989), and Faure (1991), the slightly curved reaction paths of potassium feldspar dissolving in pure water (originally illustrated by Helgeson *et al.*, 1969) have been redrawn as straight lines. These redrawn paths leave the student with the impression that reaction paths are normally straight lines. The example in the book by Faure (1991) includes a calculation of the slope of a reaction path, but the equation used is incorrect. As a result, the line and its calculated slope also are incorrect. The book by Drever (1988) is confusing because both linear (Chapter 7) and curved reaction paths (Chapter 14) are presented for the same feldspar example.

Reaction paths typically are curved lines in the log-log space of activity diagrams depicting mineral stability equilibria. Furthermore, a path and its degree of curvature are very sensitive to the initial pH and solution composition. Unfortunately, the dependence of a reaction path on the starting composition of the solution is not discussed in any of these textbooks. Furthermore, Richardson and McSween (1989) suggest that reaction path calculations are cumbersome, requiring complex programs that run on mainframe computers. In fact, examples of reaction paths of feldspar dissolving in water at relatively low pH can be illustrated quite simply using a desktop computer and a spreadsheet program.

The first goal of this paper is to show that reaction path modeling can be introduced to students using simple calculations easily performed with the help of commercial spreadsheet programs. The second objective is to illustrate the curvature of the reaction path and its dependence on the initial fluid composition. Third, we show how aqueous species may be included in the calculations using mathematical programs such as Maple (Char *et al.*, 1991) or Mathematica (Wolfram, 1991). Finally, the calculated reaction paths (for both closed and open systems) are compared and shown to be very similar to the paths obtained using the sophisticated modeling program MPATH.

[1] Present address: Southwest Research Institute, CNWRA, 6220 Culebra Road, San Antonio, Texas 78228-5166.

DEFINITION OF A REACTION PATH

The reaction of a mineral with an aqueous solution results in the release of solute species into solution with the possible formation of one or more solid products. The successive changes in the composition of the solution with continued reaction are referred to as a reaction path. A reaction path may be parameterized by the reaction progress variable, ξ (De Donder, 1920; Prigogine and Defay, 1967). The variable, ξ, is proportional to the amount of reactant mineral dissolved and defines the extent of reaction.

One useful way of depicting a reaction path is to project the solution composition on a log-log activity diagram. These diagrams show which minerals are stable for a given composition of the aqueous solution. The construction of such diagrams is discussed in detail elsewhere (e.g., Garrels and Christ, 1965; Drever, 1988; Richardson and McSween, 1989; Faure, 1991).

DISSOLUTION OF MICROCLINE IN A CLOSED SYSTEM

The dissolution of potassium feldspar (microcline) in a closed system is a standard textbook example depicting a weathering reaction. Such a closed system may be represented by a laboratory experiment where microcline powder is allowed to react with a well-mixed HCl solution in a closed beaker held at constant temperature and pressure.

Two assumptions are required to reduce the number of variables describing the reaction path. First, it is assumed that no aluminum is transferred from the solid to the aqueous phase or vice versa. This assumption allows mineral reactions to be written that are balanced on aluminum. The second assumption is that of partial equilibrium. While the system is not in equilibrium with the dissolving feldspar, all secondary minerals are assumed to be in instantaneous equilibrium with the aqueous solution. Although these two assumptions are strictly speaking incompatible, as we discuss in the last section, nevertheless they provide a useful approximation of the reaction path for a certain compositional range.

With these assumptions the dissolution of microcline in a closed system may be described in a simple fashion. As a first example, we take the initial composition of the aqueous solution—corresponding to an acidic soil solution—to be: pH = 4.0, $[K^+] = [H_4SiO_4] = 10^{-6}$ moles per kg of solution. The composition of this solution plots in the gibbsite stability field (point A″ in Figure 1). Due to the first assumption, the solution is saturated with respect to gibbsite. Therefore, microcline initially dissolves while gibbsite precipitates according to the reaction:

$$\underset{\text{microcline}}{KAlSi_3O_8} + H^+ + 7\,H_2O$$

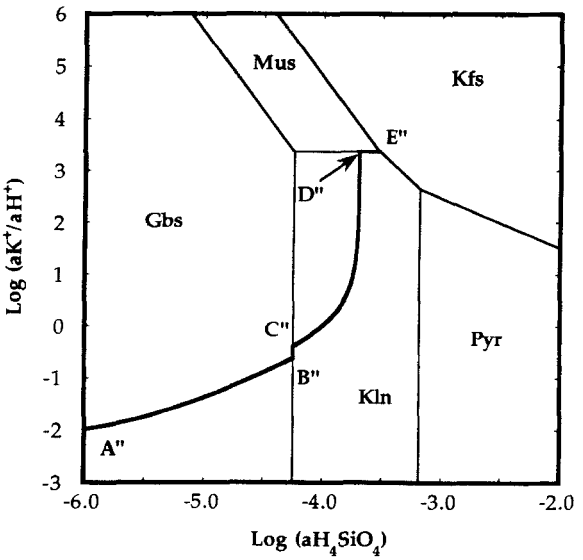

Figure 1. Reaction paths for the weathering of microcline in a closed system at 25°C and 1 bar, as obtained from the spreadsheet calculations presented in Table 1. The stability fields of gibbsite (Gbs), kaolinite (Kln), muscovite (Mus), microcline (Kfs), and pyrophyllite (Pyr) are shown in the log-log activity diagram. The thermodynamic data for the construction of the diagram is given in Table 3. The initial pH of the HCl solution is 4.0. The composition of the solution and the amounts of minerals present at each labeled point are given in Table 2. Note that concentrations have been used as approximations for activities to calculate the points plotted in this figure.

$$\rightleftharpoons \underset{\text{gibbsite}}{Al(OH)_3} + K^+ + 3\,H_4SiO_4. \qquad (1)$$

Because the solutions in this example are sufficiently dilute, the activity coefficients of the aqueous species in solution are near unity (Garrels and Christ, 1965). Therefore, the evolution of the solution can be plotted on the log-log activity diagram shown in Figure 1 using aqueous species concentrations as proxies for activities without introducing significant error. As reaction 1 proceeds, the composition of the aqueous solution evolves along reaction path $\overline{A''B''}$ (Figure 1) with both $[K^+]/[H^+]$ and $[H_4SiO_4]$ increasing. The reaction continues until equilibrium with kaolinite is achieved at point B″. Beyond this point, gibbsite is unstable and begins to dissolve as kaolinite starts to precipitate. If partial equilibrium is to be maintained, all gibbsite is transformed into kaolinite according to the reaction:

$$\underset{\text{microcline}}{KAlSi_3O_8} + 2\,\underset{\text{gibbsite}}{Al(OH)_3} + H^+ \rightleftharpoons 1.5\,\underset{\text{kaolinite}}{Al_2Si_2O_5(OH)_4} + K^+ + 0.5\,H_2O. \qquad (2)$$

which restricts the reaction path to the boundary between the stability-fields of gibbsite and kaolinite. Along

https://doi.org/10.1346/CCMN.1994.0420210 Published online by Cambridge University Press

this boundary $[K^+]/[H^+]$ continues to increase while $[H_4SiO_4]$ remains unchanged.

Reaction 2 stops once all of the gibbsite has been dissolved (point C″ in Figure 1). At this point $[H_4SiO_4]$ can once again increase, and further dissolution of microcline leads to the precipitation of kaolinite according to the reaction:

$$\underset{\text{microcline}}{KAlSi_3O_8} + H^+ + 4.5\,H_2O \rightleftharpoons 0.5\,\underset{\text{kaolinite}}{Al_2Si_2O_5(OH)_4} + K^+ + 2\,H_4SiO_4. \quad (3)$$

The reaction path encounters the muscovite field at point D″. Here, kaolinite begins to dissolve in addition to microcline as muscovite precipitates. As long as kaolinite is present the reaction path must not leave the horizontal boundary between the kaolinite and the muscovite stability-fields. The reaction:

$$\underset{\text{microcline}}{KAlSi_3O_8} + \underset{\text{kaolinite}}{Al_2Si_2O_5(OH)_4} + 3\,H_2O \rightleftharpoons \underset{\text{muscovite}}{KAl_3Si_3O_{10}(OH)_2} + 2\,H_4SiO_4 \quad (4)$$

proceeds until equilibrium is reached with microcline (reaction path $\overline{D''E''}$, Figure 1). Point E″ corresponds to simultaneous equilibrium of all three minerals microcline, kaolinite and muscovite with the aqueous solution.

Calculation of the reaction path

In the above description, the reaction path $\overline{A''B''C''D''E''}$ (Figure 1) has been divided into the four segments $\overline{A''B''}$, $\overline{B''C''}$, $\overline{C''D''}$, and $\overline{D''E''}$, each of which is characterized by the approximate overall reactions given in Eqs. 1, 2, 3, and 4, respectively. The reaction coefficients in these equations describe in what proportions the different species are released into solution or are precipitated as the reaction proceeds. In a first, very simple approach, the dissociation of H_2O and H_4SiO_4 are neglected. The composition of the aqueous phase for a finite extent of reaction is then given by:

$$[H^+] = [H^+]_0 + u\xi \quad (5)$$

$$[K^+] = [K^+]_0 + v\xi \quad (6)$$

$$[H_4SiO_4] = [H_4SiO_4]_0 + w\xi, \quad (7)$$

where $[H^+]_0$, $[K^+]_0$, and $[H_4SiO_4]_0$ represent the initial concentrations (in moles per kg of solution) of the aqueous species at the starting point of each reaction path segment. As mentioned above, because the solutions considered in this example are sufficiently dilute, concentrations may be used instead of activities without introducing significant error. The quantities $[H^+]$, $[K^+]$, and $[H_4SiO_4]$ give the composition of the aqueous solution for a given value of the reaction progress variable, ξ (given in units of moles per kg of solution). The constants u, v, and w refer to the reaction coefficients of their respective aqueous species, where, by convention, the coefficients of products and reactants of reaction are taken to be positive and negative, respectively. For example, in reaction 1, $u = -1$, $v = 1$, and $w = 3$.

The amount of each mineral that has reacted (N_m^ξ, given in moles per kg of solution) is calculated in a similar fashion according to the expression:

$$N_m^\xi = N_m^0 + r\xi, \quad (8)$$

where N_m^0 refers to the amount of the mth mineral present at the starting point of each reaction path segment (in moles per kg of solution) and r is the reaction coefficient for the mineral. For example, in the case of reaction 3 $r = -1$ for microcline and $r = 0.5$ for kaolinite. Again, ξ is the reaction progress variable.

From Eqs. 5–8, a reaction path for the microcline example discussed above is easily evaluated using a spreadsheet program (e.g., Excel). For each segment of the reaction path, an Excel (or some other) spreadsheet similar to Table 1 must be constructed. For example, in Table 1, calculations for the reaction path segment $\overline{C''D''}$ in Figure 1 are displayed. In this table, the concentrations of the aqueous species and the amounts of precipitated or dissolved minerals are calculated in different columns. The first row contains the initial composition of the solution as well as the amounts of minerals initially present at point C″. In each following row, the reaction is allowed to proceed for a small increment (i.e., step), $\Delta\xi$ artibrarily selected as the value shown in column E (Table 1). For this and all similar reaction path tables, in order to plot the reaction path on a log-log activity diagram, $\log([K^+]/[H^+])$ and $\log([H_4SiO_4])$ are calculated in each row. If the reaction path reaches the border of a stability field or if an unstable mineral is completely consumed, the next stage of the reaction path is calculated with a new spreadsheet containing the appropriate reaction coefficients. The initial values in the spreadsheet for the new reaction path segment are taken from the last row of the previous spreadsheet.

The reaction path shown in Figure 1 was evaluated using the approximate form of the reactions balanced on aluminum (Eqs. 1–4) with the help of Excel spreadsheets, such as the one shown in Table 1. Results of these calculations (values corresponding to points A″–E″) are given in Table 2. Clearly, segments of this path that traverse mineral stability fields are curved in log-log activity space. This is in contrast with the equations for the calculation of the slopes of the (straight) reaction path segments given by Faure (1991), which are incorrect (see Appendix A).

https://doi.org/10.1346/CCMN.1994.0420210 Published online by Cambridge University Press

Table 1. Sample Excel spreadsheet for the calculation of reaction path segment $\overline{C''D''}$ (Figure 1).

	A	B	C	D	E	G	F
1	$[H^+]$	$[K^+]$	$[H_4SiO_4]$	kaolinite	$\Delta\xi$ (step)	log ($[H_4SiO_4]$)	log ($[K^+]/[H^+]$)
2	7.24E−05	2.89E−05	5.68E−05	1.40E−5	7.46E−07	=logC2	=log (B2/A2)
3	=A2− 1*E2	=B2+ 1*E2	=C2+ 2*E2	=D2+ 0.5*E2		=logC3	=log (B3/A3)
4	=A3− 1*E2	=B3+ 1*E2	=C3+ 2*E2	=D3+ 0.5*E2		=logC4	=log (B4/A4)
...	...	...	...	...	...	...	...
99	=A98− 1*E2	=B98+ 1*E2	=C98+ 2*E2	=D98+ 0.5*E2		=logC98	=log (B98/A98)

Columns A, B, and C display the concentrations of the aqueous species in moles/kg of solution and the Excel equations necessary to generate them. Column D records the moles of kaolinite formed by Reaction 3. Columns G and F provide variables that allow the reaction path to be plotted in the log-log activity diagram shown in Figure 1. Field E2 (referred to as E2 in formulas) defines the arbitrarily selected reaction increment $\Delta\xi$. This step value has been adjusted so that row 99 gives the values for point D″, where the reaction path meets the boundary of the kaolinite-stability field. The factors −1, 1, 2, and 0.5 beginning in row 3 of columns A–D are the respective reaction coefficients from reaction 3. Row 2 contains the concentrations of aqueous species and moles of minerals in the system for this reaction path segment (point C″, Figure 1). These values have been calculated with an analogue of this spreadsheet for reaction path segment $\overline{B''C''}$.

The influence of the dissociation of H_4SiO_4 and H_2O

The pH-values obtained from the simple reaction path calculations presented above are only approximate because the dissociation of H_2O and H_4SiO_4 has been neglected. As the pH increases above 7, the dissociation of H_2O and H_4SiO_4 becomes an important source of hydrogen ions and, thus, counters the increase in pH produced by the weathering of silicates as shown in Reactions 1–3. In addition to its effect on the pH, the formation of $H_3SiO_4^-$ increases the number of aqueous silica species in solution, thereby enhancing the release of silica to solution by mineral dissolution.

To provide a more accurate description of the system under consideration these additional species have to be included in Eqs. 5 and 7, which become:

$$[H^+] = [H^+]_0 + ([OH^-] - [OH^-]_0) + ([H_3SiO_4^-] - [H_3SiO_4^-]_0) + u\xi \quad (9)$$

$$[H_4SiO_4] = [H_4SiO_4]_0 - ([H_3SiO_4^-] - [H_3SiO_4^-]_0) + w\xi. \quad (10)$$

Again, u and w are the appropriate reaction coefficients; and the subscript, $_0$, denotes initial concentrations. Because the dissociation reactions of H_2O and H_4SiO_4 release one proton per negatively charged ligand, $[OH^-] - [OH^-]_0$ and $[H_3SiO_4^-] - [H_3SiO_4^-]_0$ give the concentrations of H^+ derived from dissociated molecules of water and H_4SiO_4, respectively. In addition, the following equilibria have to be considered:

$$[H^+][H_3SiO_4^-] = [H_4SiO_4]K_{si} \quad (11)$$

$$[H^+][OH^-] = K_w, \quad (12)$$

Values for K_w and K_{si} are given in Table 3. More dissociated silica species (e.g., $H_2SiO_4^{2-}$) are ignored because they are important only if the pH is higher than 11 (Stumm and Morgan, 1981).

Substituting Eqs. 11 and 12 into Eqs. 9 and 10 yields the following equations:

$$[H^+] = [H^+]_0 + K_w(1/[H^+] - 1/[H^+]_0) + K_{si}([H_4SiO_4]/[H^+] - [H_4SiO_4]_0/[H^+]_0) + u\xi \quad (13)$$

$$[H_4SiO_4] = [H_4SiO_4]_0 - K_{si}([H_4SiO_4]/[H^+] - [H_4SiO_4]_0/[H^+]_0) + w\xi. \quad (14)$$

The commercial mathematical package Maple was used for the reaction path calculations based on the simultaneous solution of Eqs. 6, 13, and 14 (see Appendix B). Again, each segment of the reaction path was calculated separately using the appropriate reaction coefficients. The results of these calculations for the example discussed above are given in Table 2 as A′, B′, C′, D′, and E′, which correspond to points A″, B″, C″, D″, and E″. The obtained reaction path is almost identical to the reaction path shown in Figure 1.

For the calculation of the reaction path segment $\overline{D'E'}$ (corresponding to $\overline{D''E''}$ in Figure 1) the coefficients from Eq. 4 cannot be used. Since the H_4SiO_4 released in the reaction is now allowed to dissociate, it provides a source of protons. As a consequence, values of $\log([K^+]/[H^+])$ would diminish and the reaction path would move from the muscovite-kaolinite boundary down into the kaolinite field. However, Reaction 3

https://doi.org/10.1346/CCMN.1994.0420210 Published online by Cambridge University Press

Table 2. Summary of amounts of minerals reacted and concentrations of the aqueous species.

	Gbs	Kln	Mus	$[K^+]$	pH	$[H_4SiO_4]$	$[Al]_{total}$
A	0	0	0	1.00E−06	4.00	1.00E−06	1.00E−12
A′	0	0	0	1.00E−06	4.00	1.00E−06	
A″	0	0	0	1.00E−06	4.00	1.00E−06	
B	1.55E−05	0	0	1.95E−05	4.14	5.66E−05	3.02E−06
B′	1.86E−05	0	0	1.96E−05	4.09	5.68E−05	
B″	1.86E−05	0	0	1.96E−05	4.09	5.68E−05	
C	0	1.23E−05	0	2.80E−05	4.18	5.74E−05	2.29E−06
C′	0	1.40E−05	0	2.89E−05	4.14	5.68E−05	
C″	0	1.40E−05	0	2.89E−05	4.14	5.68E−05	
D	0	5.07E−05	0	1.03E−04	7.36	2.04E−04	2.68E−09
D′	0	5.01E−05	0	1.01E−04	7.37	2.02E−04	
D″	0	5.00E−05	0	1.01E−04	7.37	2.01E−04	
E	0	3.98E−06	4.69E−05	1.03E−04	7.36	2.98E−04	1.82E−09
E′	0	1.52E−06	4.85E−05	1.01E−04	7.36	2.99E−04	
E″	0	1.17E−06	4.88E−05	1.01E−04	7.37	2.99E−04	
F′	0	0	0	1.00E−07	5.00	1.00E−06	1.00E−12
G	1.52E−05	0	0	1.55E−05	8.48	4.50E−05	1.21E−07
G′	1.66E−05	0	0	1.67E−05	8.48	4.41E−05	
H	0	0	7.64E−05	1.56E−05	8.49	4.52E−05	1.22E−07
H′	0	0	8.29E−05	1.67E−05	8.48	4.41E−05	
I	0	0	2.10E−05	4.23E−05	9.08	1.08E−04	9.01E−08
I′	0	0	1.38E−05	4.97E−05	9.01	1.07E−04	
K′	0	0	0	1.00E−09	7.00	1.00E−06	1.00E−12
L	1.24E−05	0	0	1.27E−05	8.90	3.48E−05	3.16E−07
L′	1.56E−05	0	0	1.56E−05	8.92	3.21E−05	
M	0	0	6.22E−06	1.28E−05	8.90	3.51E−05	3.15E−07
M′	0	0	7.78E−06	1.56E−05	8.92	3.21E−05	
N	0	0	2.03E−05	4.08E−05	9.20	9.89E−05	1.20E−07
N′	0	0	1.37E−05	5.10E−05	9.16	9.47E−05	

Minerals reacted are provided in moles per kg of solution and concentrations of the aqueous species are given in moles per kg of solution (or in activities when calculated with MPATH) for the labeled points in Figures 1 and 2. Points A″–E″ correspond to points obtained from the spreadsheet calculations discussed in the text and are shown in Figure 1. Points A′–N′ are calculated with Maple as presented in the text. These points correspond to points A–N calculated with MPATH and shown in Figure 2. (Gbs = gibbsite, Kln = kaolinite, Mus = muscovite, Al = total dissolved aluminum.)

Table 3. Reactions involved in the weathering of microcline at 25°C and 1 bar as used in the program MPATH.

Mineral hydrolysis reactions:	log K (25°C, 1 bar)
$Al(OH)_3 + 3H^+ = Al^{3+} + 3H_2O$	6.796
$Al_2Si_2O_5(OH)_4 + 6H^+ = 2Al^{3+} + 2H_4SiO_4 + H_2O$	5.101
$KAl_3Si_3O_{10}(OH)_2 + 10H^+ = K^+ + 3Al^{3+} + 3H_4SiO_4$	11.022
$KAlSi_3O_8 + 4H^+ + 4H_2O = K^+ + Al^{3+} + 3H_4SiO_4$	−1.130
Aqueous speciation reactions:	**log K (25°C, 1 bar)**
$H_2O = H^+ + OH^-$	−14.0
$H_4SiO_4 = H_3SiO_4^- + H^+$	−9.57
$Al(OH)^{2+} + H^+ = Al^{3+} + H_2O$	5.011
$Al(OH)_2^+ + 2H^+ = Al^{3+} + 2H_2O$	10.099
$Al(OH)_3(aq) + 3H^+ = Al^{3+} + 3H_2O$	16.158
$Al(OH)_4^- + 4H^+ = Al^{3+} + 4H_2O$	22.201

The equilibrium constants are taken from the EQ3/6 database (Wolery and Daveler, 1992). These constants are thermodynamic constants based on activities (e.g., Stumm and Morgan, 1981). Activities of pure solids and liquids are taken to be 1 and activities of aqueous species are referenced to infinite dilution.

forces the path back to the phase boundary. For 100 incremental steps of Eq. 4, it takes approximately 1.2 steps (of the same increment) of Eq. 3 to keep the reaction path on the muscovite-kaolinite boundary (Appendix C). The approximate overall reaction can be written as sum of Eq. 4 and 0.012 times Eq. 3

$$1.012\underset{\text{microcline}}{KAlSi_3O_8} + 0.994\underset{\text{kaolinite}}{Al_2Si_2O_5(OH)_4} + 3.054H_2O + 0.012H^+ = \underset{\text{muscovite}}{KAl_3Si_3O_{10}(OH)_2} + 2.024H_4SiO_4 + 0.012K^+. \quad (15)$$

Table 2 shows that the reaction path $\overline{A''B''C''D''E''}$ (calculated by neglecting all speciation reactions) agrees remarkably well with the path that would be described by $\overline{A'B'C'D'E'}$ (which includes the speciation of H_2O and H_4SiO_4). The simplifications used in the first approach, therefore, were reasonable for a solution with an initial pH of 4.0.

For higher initial pH values, however, the influence

https://doi.org/10.1346/CCMN.1994.0420210 Published online by Cambridge University Press

of speciation reactions in the aqueous solution becomes more important and cannot be neglected. The calculations using Maple presented above do account for the most important speciation reactions and can, therefore, be applied to microcline dissolution in aqueous solutions with higher initial pH. Reaction paths for microcline dissolution in solutions with initial pH of 5 and 7 have been calculated using the Maple-approach. The results are given in Table 2 as points F′, G′, H′, I′ and K′, L′, M′, N′, respectively. The obtained reaction paths are almost identical to the paths $\overline{FGHI}$ and $\overline{KLMN}$ shown in Figure 2. These reaction paths do not enter the kaolinite field but cross the gibbsite-muscovite boundary (see Figure 2). In the closed system at that boundary, all gibbsite must be converted to muscovite before the reaction path can leave the boundary. Although Drever (1988) has suggested that the reaction path should move along the gibbsite-muscovite boundary, this is not possible. Assuming local equilibrium, the following reaction takes place:

$$\underset{\text{gibbsite}}{2\,Al(OH)_3} + \underset{\text{microcline}}{KAlSi_3O_8} \rightleftharpoons \underset{\text{muscovite}}{KAl_3Si_3O_{10}(OH)_2} + 2\,H_2O. \quad (16)$$

As muscovite is produced by this reaction, the concentrations of aqueous species remain constant and the position of the reaction path is fixed.

Once all the gibbsite has been consumed, muscovite continues to be produced from the dissolution of microcline as follows:

$$\underset{\text{microcline}}{3\,KAlSi_3O_8} + 2\,H^+ + 12\,H_2O \rightleftharpoons \underset{\text{muscovite}}{KAl_3Si_3O_{10}(OH)_2} + 2\,K^+ + 6\,H_4SiO_4. \quad (17)$$

This reaction corresponds to the points H′, I′ and M′, N′ in Table 2 and the reaction path segments $\overline{H'I'}$ and $\overline{M'N'}$ represented by these points. These two path segments are approximated by those corresponding to $\overline{HI}$ and $\overline{MN}$ in Figure 2.

The solubility of aluminum

In the foregoing calculations, the concentration of aluminum in solution was assumed to be negligible. As mentioned earlier, this assumption is incompatible with the concept of partial equilibrium, which demands equilibrium between all aqueous species in solution and secondary mineral alteration products. Equilibrium is defined by the solubility product of the minerals. For example, in the stability field of kaolinite, the solubility product (K_{sp}) for the reaction shown in Table 3 can be written as:

$$K_{sp} = \frac{[Al^{3+}]^2\,[H_4SiO_4]^2}{[H^+]^6}. \quad (18)$$

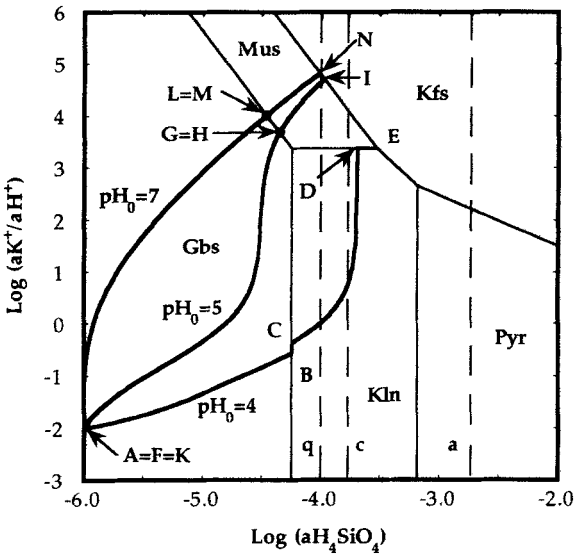

Figure 2. Reaction paths for the weathering of microcline in a closed system, as calculated by MPATH. The mineral stability fields are the same as in Figure 1. Saturation lines for quartz (q), chalcedony (c), and amorphous silica (a) are also indicated. The precipitation of quartz and chalcedony is ignored in the calculations because of kinetic inhibitions and slow nucleation and crystallization rates (Stumm and Morgan, 1981). The initial pH values of the HCl solutions (pH_0) are 4.0 (path $\overline{ABCDE}$), 5.0 (path $\overline{FGHI}$), and 7.0 (path $\overline{KLMN}$). The composition of the solution and the amounts of minerals present at each labeled point are given in Table 2. The points in this figure are calculated from activities. Calculations with the program Maple presented in the text yield almost identical reaction paths (Table 2).

Clearly, the concentration of Al^{3+} increases with decreasing pH (at constant $[H_4SiO_4]$) and decreases with increasing $[H_4SiO_4]$ (at constant pH). In addition, the speciation of aqueous aluminum (Table 3) controls the concentration of total dissolved aluminum. Typically, the solubility of aluminum hydroxides or aluminum silicates increases toward both high and low pH with a minimum between approximately pH 5 and 8 (e.g., Drever, 1988).

A reaction path that includes aluminum solubility equilibria and the speciation of dissolved constituents can be readily calculated using geochemical modeling codes. In the present study the computer program MPATH (Lichtner, 1988, 1992) was used to perform these calculations. The program MPATH takes into account the speciation reactions given in Table 3. Mineral reactions taking place in the system are also described by the hydrolysis reactions shown in the table, some or all of which may take place simultaneously. For the weathering of feldspar, the concentration of total dissolved aluminum, as obtained from MPATH calculations, is given in Table 2 along with computed values for the pH, concentrations of K^+ and H_4SiO_4, as well as the moles of gibbsite, kaolinite, and mus-

https://doi.org/10.1346/CCMN.1994.0420210 Published online by Cambridge University Press

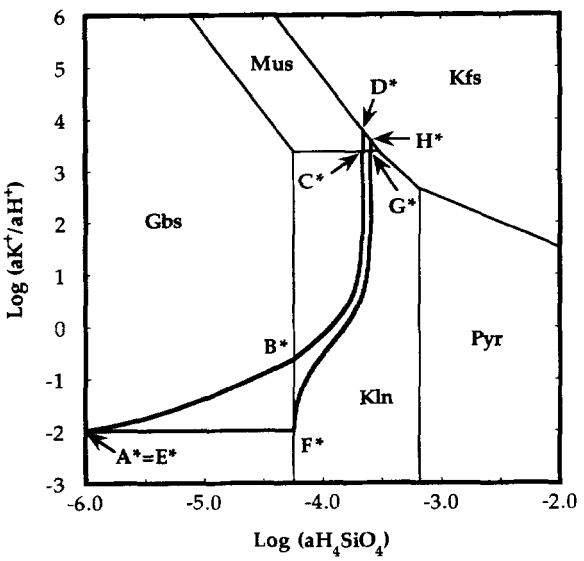

Figure 3. Reaction paths for the weathering of microcline in an open system. The figure is plotted from an Excel spreadsheet similar to the one initially discussed for the closed system example presented in the text. The initial pH of the solution (points A* and E*) is 4.0. Reaction path $\overline{A^*B^*C^*D^*}$ characterizes the initial stage of weathering where microcline is present throughout the whole soil profile. Reaction path $\overline{E^*F^*G^*H^*}$ is followed during later stages of weathering where a zoned soil profile has developed and no more microcline is present in the upper layers.

covite precipitated or dissolved at points A–M. The locations of points A–M are—together with the whole reaction path—depicted in Figure 2. Excellent agreement is obtained between values calculated by MPATH and the Maple calculations for all reaction paths reported, and good agreement may be seen between the MPATH calculations and Excel spreadsheet calculations for the reaction path at an initial pH of 4.0.

As shown in Table 2, the initial aluminum concentration chosen in the MPATH calculations (point A) was very low such that, at the beginning, microcline dissolves congruently until gibbsite saturation is reached. In the simplified examples discussed above, the initial solution was assumed to be saturated with respect to gibbsite, so gibbsite precipitated from the beginning of the reaction (points A″ and A′), which explains why more gibbsite is present at the points B′ and B″ than at B (Table 2). Between points B and D, the amount of dissolved aluminum decreases markedly, which can be attributed to the increase of the initially low pH to an intermediate value. Between points D and E, the pH remains constant, but the amount of dissolved aluminum still decreases. This is due to the increasing concentration of H_4SiO_4 (Eq. 18).

As shown above, including aqueous aluminum in the model leads to overall reactions that are no longer balanced on aluminum, but allow Al^{3+} to go into or out of the aqueous phase. The amount of Al^{3+} going into or out of the aqueous phase is not constant over a whole segment of the reaction path because it depends on the pH (and also on $[H_4SiO_4]$ if the secondary minerals are aluminosilicates), which varies continuously along the path. The reaction coefficient for Al, therefore, changes along one segment of the reaction path. As a consequence, in order to retain charge balance, other reaction coefficients may change, too. For this reason the speciation of aqueous aluminum cannot be included in simple calculations as presented above.

THE FORMATION OF A SOIL PROFILE: AN OPEN SYSTEM

To describe geological weathering phenomena, the above treatment of closed systems must be extended to open systems. As an example, consider the weathering of a homogeneous porous rock by a fluid (e.g., rainwater) percolating through the rock. The stream of fluid may be thought of as a series of individual fluid packets moving downward through the rock. As an approximation, diffusion and hydrodynamic dispersion are neglected. The system is open because of the movement of the fluid packet: The solid reaction products form precipitates that remain at the site of precipitation, while the fluid moves further downward along the flowpath.

For simplicity, consider an unweathered rock consisting entirely of microcline. The initial composition of the fluid is the same as in the closed system of pH = 4.0 discussed above. Given the excellent agreement between the Excel and MPATH calculations for solutions of pH = 4.0, the open system weathering of microcline was calculated using the simple Excel spreadsheet scheme described above for closed systems. Consider the first packet of fluid. The first reaction to occur is the incongruent dissolution of microcline by precipitating gibbsite (Eq. 1; path $\overline{A^*B^*}$ in Figure 3). As this reaction takes place, the fluid is moving downward, producing a gibbsite-bearing zone along the flow path. As the solution becomes saturated with respect to kaolinite (point B* in Figure 3), gibbsite formation stops and the weathering of microcline continues according to Eq. 3 (path $\overline{B^*C^*}$, Figure 3). A kaolinite-bearing zone is produced. When the aqueous solution becomes saturated with respect to muscovite (point C*, Figure 3), kaolinite stops precipitating and muscovite is formed instead (Eq. 17). Finally, equilibrium between the fluid and microcline (unweathered rock) is obtained (point D*, Figure 3).

The first packet of fluid has produced a zoned weathering profile, each zone containing a tiny amount of different reaction products. The reaction path is useful to illustrate the sequence of the secondary minerals precipitated (Figure 3). At this stage, however, no information is obtained about the thickness of the different reaction zones. Assuming a constant flow velocity, the thickness of a reaction zone depends on the

time needed by the fluid to evolve along the particular segment of the reaction path. If microcline is dissolving at a constant rate, this time is proportional to ξ. In Figure 4, cumulative amounts of precipitated minerals are plotted against ξ. The amounts of minerals formed are tiny, but these numbers account only for one liter (one packet) of fluid. Each following packet will increase the moles of secondary minerals the same amount, until all of the original rock has reacted and a zoned weathering profile is obtained as shown on the right hand side of Figure 4. The profile consists of an uppermost zone containing gibbsite, followed by a thick kaolinite zone with a tiny muscovite zone overlying the fresh rock. As this soil profile is weathered further, the fluid will react with the particular mineral characterizing each zone and evolve along the reaction path outlined below.

During further fluid infiltration, no reaction takes place in the gibbsite zone because of the assumption that the reactions are balanced on aluminum and the initial fluid is taken to be saturated with respect to gibbsite. In the kaolinite zone, however, kaolinite will dissolve while gibbsite precipitates according to:

$$\underset{\text{kaolinite}}{Al_2Si_2O_5(OH)_4} + 5\,H_2O \rightleftharpoons 2\,\underset{\text{gibbsite}}{Al(OH)_3} + 2\,H_4SiO_4, \quad (19)$$

The corresponding reaction path is represented by $\overline{E^*F^*}$ in Figure 3. The reaction stops when the solution becomes saturated with respect to kaolinite. The fluid then flows through the tiny muscovite zone, which is quantitatively unimportant (Figure 4) and reaches the fresh "microcline rock" being in equilibrium with kaolinite (point F*, Figure 3). Here microcline dissolves, while kaolinite is precipitated (Eq. 3; reaction path $\overline{F^*G^*}$ in Figure 3). At point G*, this is followed by the precipitation of muscovite (Eq. 17; reaction path $\overline{G^*H^*}$ in Figure 3). In this second stage of weathering, characterized by reaction path $\overline{E^*F^*G^*H^*}$ (Figure 3), the sequence of mineral zones established during the initial stage of weathering has not changed, but each zone has been extended downward. Therefore, any further weathering proceeds according to reaction path $\overline{E^*F^*G^*H^*}$ (Figure 3).

The reaction paths shown in Figure 3 have been obtained using the initial simple Excel spreadsheet calculations discussed for Eqs. 1, 3, 17, and 19 with the same initial fluid compositions as in the closed system examples for fluids with initial pH = 4.0. Comparison with reaction paths calculated by the full-scale program MPATH for a similar weathering situation (Lichtner, 1988) shows that the simple "spreadsheet" approach yields a reasonable approximation of the fully calculated path at this pH. As the pH increases, however, similar calculations incorporating simple speciation terms using programs such as Maple and Mathematica, can still provide close approximations of results obtained from the more sophisticated geochemical modeling codes that are presently available.

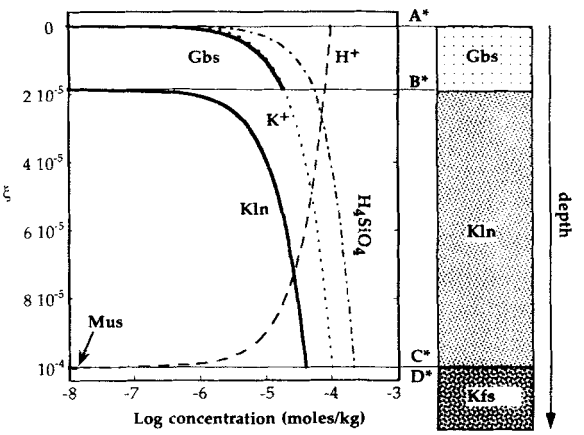

Figure 4. Cumulative amounts of minerals (solid curved lines) and concentrations of aqueous species (dashed curved lines) during the course of the open system reactions along $\overline{A^*B^*C^*D^*}$ in Figure 3. The diagram is obtained from the same spreadsheet calculations used for Figure 3. As the reactions progress, variable ξ (given in moles/kg of solution) increases from zero, first gibbsite (Gbs), then kaolinite (Kln), and finally a tiny amount of muscovite (Mus) is formed before the fluid equilibrates with the unweathered rock consisting of microcline (Kfs). Although, for the calculations of the individual curves (segments), the reaction progress variable, ξ, is taken to start from zero for each, in order to obtain this plot it had to be summed over the whole reaction path. Horizontal lines labeled A*, B*, C*, and D* correspond to the respective points in Figure 3. Assuming a constant fluid flow rate and a constant reaction rate for microcline, the diagram may be converted into relative thicknesses resulting in a depth profile of mineral zones as shown to the right. Note that the muscovite zone is too thin to be represented in the depth profile.

CONCLUSIONS

The calculation of mineral weathering reaction paths can be introduced easily using the textbook example of microcline dissolving in an aqeuous solution in a closed system. The calculations are simplified by assuming that aluminum is conserved by mineral reactions and that partial equilibrium is maintained, ignoring the speciation of Al, H_2O, and H_4SiO_4. For acidic aqueous solutions, these calculations yield reasonable results and demonstrate that reaction paths are curved when depicted in log-log activity diagrams.

Speciation reactions in the fluid can be gradually included in the calculations using available commercial mathematical equation solving programs. Reaction paths have been calculated using three different initial pH values to show that the paths are highly dependent upon the initial composition and, particularly, the pH of the solution. The reaction paths obtained in this manner agree well with those calculated with more sophisticated, comprehensive geochemical modeling programs such as MPATH. In addition, reaction path

https://doi.org/10.1346/CCMN.1994.0420210 Published online by Cambridge University Press

calculations can be extended to open systems to show, for example, the mineralogical evolution of soil profiles.

ACKNOWLEDGMENTS

This work was partly funded by the Swiss National Science Foundation (Grant 21-30207.90). The review by B. Ransom helped greatly to improve an earlier version of the manuscript.

REFERENCES

Berner, E. K. and Berner, R. A. (1987) *The Global Water Cycle:* Prentice Hall, Englewood Cliffs, N.J., 397 pp.

Char, B. W., Geddes, K. O., Gonnet, G. H., Leong, B. L., Monagan, M. B., and Watt, S. M. (1991) *Maple V Language Reference Manual:* Springer, New York, 267 pp.

De Donder, T. (1920) *Leçons de Thermodynamique et de Chimie Physique:* F.H. van den Dungen and G. van Lerberqhe, Paris.

Drever, J. I. (1988) *The Geochemistry of Natural Waters,* 2nd ed., Prentice Hall, Englewood Cliffs, N.J., 388 pp.

Faure, G. (1991) *Principles and Applications of Inorganic Geochemistry:* Macmillan, New York, 626 pp.

Garrels, R. M. and Christ, C. L. (1965) *Solutions, Minerals and Equilibria:* Freeman, Cooper and Co., San Francisco, 450 pp.

Helgeson, H. C. (1968) Evaluation of irreversible reactions in geochemical processes involving minerals and aqueous solutions. I. Thermodynamic relations: *Geochim. Cosmochim. Acta* **32,** 853–877.

Helgeson, H. C., Garrels, R. M., and MacKenzie, F. T. (1969) Evaluation of irreversible reactions in geochemical processes involving minerals and aqueous solutions. II. Applications: *Geochim. Cosmochim. Acta* **33,** 455–481.

Lichtner, P. C. (1988) The quasistationary state approximation to coupled mass transport and fluid-rock interaction in a porous medium: *Geochim. Cosmochim. Acta* **52,** 143–165.

Lichtner, P. C. (1992) Time-space continuum description of fluid/rock interaction in permeable media: *Water Resources Research* **28,** 3135–3155.

Plummer, L. N., Prestemon, E. C., and Parkhurst, D. L. (1991) An interactive code (NETPATH) for modelling *NET* geochemical reactions along a flow path: *U.S. Geological Survey Water-Resources Investigations Report* **91-4078,** 227 pp.

Prigogine, I. and Defay, R. (1967) *Chemical Thermodynamics:* Longmans, Green and Co. Ltd., London, 543 pp.

Richardson, S. M. and McSween, Jr., H. Y. (1989) *Geochemistry: Pathways and Processes:* Prentice Hall, Englewood Cliffs, N.J., 488 pp.

Stumm, W. and Morgan, J. J. (1981) *Aquatic Chemistry:* 2nd ed., John Wiley & Sons, New York, 780 pp.

Wolery, T. J. and Daveler, S. A. (1992) *Calculation of Chemical Equilibrium Between Aqueous Solution and Minerals. The EQ6, a Computer Reaction Path Model of Aqueous Geochemical Systems: Theoretical Manual, User's Guide, and Related Documentation (Version 7.0):* Lawrence Livermore National Laboratory, **UCRL-MA-110662 PTIV.** 338 pp.

Wolfram, S. (1991) *Mathematica: A System for Doing Mathematics:* 2nd ed., Addison-Wesley, Redwood City, 961 pp.

(Received 10 June 1993; accepted 30 November 1993; Ms. 2384)

APPENDIX A

In a log-log activity diagram with axes $y = \log(aK^+/aH^+)$ and $x = \log(aH_4SiO_4)$, the coordinates of the points of a reaction path (as defined by Eqs. 5–7, using concentrations as an approximation of activities) are given by:

$$y = \log\left(\frac{[K^+]_0 + v\xi}{[H^+]_0 + u\xi}\right) \quad \text{(A1)}$$

$$x = \log([H_4SiO_4]_0 + w\xi). \quad \text{(A2)}$$

Solving Eq. (A2) for ξ and substituting into Eq. (A1) leads to:

$$y = \log\left(\frac{[K^+]_0 + v(10^x - [H_4SiO_4]_0)/w}{[H^+]_0 + u(10^x - [H_4SiO_4]_0)/w}\right). \quad \text{(A3)}$$

This equation does not have the form of a straight line ($y = a\,x + b$, with slope a and intercept b). Eq. A3 also shows that the reaction path is not only dependent on the initital ratio of $[K^+]/[H^+]$, but is sensitive to the magnitudes of the two variables. In Faure's book (1991), equations similar to Eqs. A1 and A2 are given; however, his equations replace terms of the form $\log(a + b)$ with $\log(a) + b$, which is incorrect.

APPENDIX B

Although other programs can be used (e.g., Mathematica), Maple, which runs on NeXT, Macintosh, Sun, and PC platforms, was used in the present study. We used version 5.01 on a Macintosh. The concentrations of $[H^+]$, $[H_4SiO_4]$, and $[K^+]$ in the solution as a function of ξ can be calculated by the command:

```
solve ({eq13, eq6, eq14}, {h, k, si});          (B1)
```

where *eq13*, *eq6*, and *eq14* should be replaced by the respective equations from the text written as follows:

```
h = h0 + kw*(1/h - 1/h0)
    + ksi*(si/h - si0/h0) + u*xi                (B2)

k = k0 + v*xi                                   (B3)

si = si0 - ksi*(si/h - si0/h0) + w*xi           (B4)
```

Here, h stands for $[H^+]$, $h0 = [H^+]_0$, $kw = K_w = 10^{-14}$, $ksi = K_{si} = 10^{-9.57}$, $si = [H_4SiO_4]$, $si0 = [H_4SiO_4]_0$, $k = [K^+]$, $k0 = [K^+]_0$, and xi stands for the reaction progress variable ξ. Moreover, in the command B1, the variables h0, k0, and si0 have to be replaced by the initial concentrations of the respective solutes at the beginning of the reaction path segment under consideration. The variables u, v, and w have to be replaced by the respective coefficients of the appropriate reaction, and xi has to be assigned an (arbitrary) value. Then Maple returns the concentrations of h, si, and k, i.e., $[H^+]$, $[H_4SiO_4]$, and $[K^+]$) for the chosen xi (i.e., ξ).

In order to plot a reaction path segment, the following sequences of commands can be used:

```
solve ({eq13, eq6, eq14}, {si, k, h}):          (B5)

x := evalf(subs(", log10(si))):                 (B6)

y := evalf(subs("", log10(k/h))):               (B7)

plot ([x, y, 0. . xi1]);                        (B8)
```

In the "solve"-command B5, the above-mentioned replacements have to be done except for xi. No value is assigned to xi. In the "plot"-command B8, *xi*1 should be replaced by the ξ-value where the reaction path segment ends. This value can be obtained using the command B1: the variable xi (ξ) is stepwise increased while checking whether the reaction path has reached the boundary of a stability field or whether some

reactand mineral is completely dissolved. For each reaction path segment, ξ is started from 0 and increased to its end value. The amounts of minerals reacted are obtained from Eq. 8.

APPENDIX C

If dissociation of H_4SiO_4 is taken into account, Eq. 4 can be written as:

$$\underset{\text{microcline}}{KAlSi_3O_8} + \underset{\text{kaolinite}}{Al_2Si_2O_5(OH)_4} + 3H_2O = \underset{\text{muscovite}}{KAl_3Si_3O_{10}(OH)_2} + 2(1 - a)H_4SiO_4 + 2aH_3SiO_4^- + 2aH^+, \quad (C1)$$

where a is the fraction of $H_3SiO_4^-$ of the total dissolved silica, which is given by:

$$\frac{a}{1 - a} = \frac{K_{Si}}{[H^+]}. \quad (C2)$$

If Reaction C1 was the only reaction taking place, the concentration of protons would increase and, therefore, the reaction path would move downward into the kaolinite stability field. However, Reaction 3 forces it back to the boundary between the two stability fields by consuming protons and releasing potassium ions. Including the species $H_3SiO_4^-$, Eq. 3 may be written as:

$$\underset{\text{Microcline}}{KAlSi_3O_8} + H^+ + 4.5\,H_2O = 0.5\,\underset{\text{Kaolinite}}{Al_2Si_2O_5(OH)_4} + K^+ + 2(1 - a)H_4SiO_4 + 2aH_3SiO_4^- + 2aH^+. \quad (C3)$$

The overall reaction taking place may then be written as the sum of Eq. C1 plus b times Eq. C3:

$$(1 + b)\underset{\text{Microcline}}{KAlSi_3O_8} + (1 - 0.5b)\underset{\text{Kaolinite}}{Al_2Si_2O_5(OH)_4} + (3 + 4.5b)H_2O = \underset{\text{Muscovite}}{KAl_3Si_3O_{10}(OH)_2} + 2(1 - a + b - ab)H_4SiO_4 + 2(a + ab)H_3SiO_4^- + (2a + 2ab - b)H^+ + bK^+. \quad (C4)$$

The coefficients of K^+ and H^+ in this reaction must be such that the value of $[K^+]/[H^+]$ at point E′ (Table 2) is preserved during the reaction. This is the case if the quotient of the coefficients is equal to the quotient of K^+ and H^+ at this point, as expressed by the equation:

$$\frac{b}{2a + 2ab - b} = \frac{[K^+]_{E'}}{[H^+]_{E'}}, \quad (C5)$$

where $[K^+]_{E'}$ and $[H^+]_{E'}$ are the respective concentrations at point E′. As an approximation we can assume that a is constant (i.e., that the pH is constant along the reaction path segment $\overline{D'E'}$) and calculate it from the pH at point E′ (Table 2) and Eq. C2. The obtained value for a is approximately 0.006. Solving Eq. C5 for b yields the factor b, which is approximately 0.012. Adding Eq. 4 and b times Eq. 3 leads to Eq. 15 given in the text.

https://doi.org/10.1346/CCMN.1994.0420210 Published online by Cambridge University Press